CHAPTER 4

Data Analysis

Open star clusters are one of the crucial objects in the structure of the Galaxy. The stars in a cluster are commonly born in the same time from the clumps of dense gas in molecular clouds, therefore they should have similar ages, distance, metallicity and kinetics. Open clusters are very helpful objects to trace star formation history, its dynamics, and Galactic structure, because they are distributed throughout and around the Galactic disk. Since they contain bright, blue stars, open clusters are testing grounds for investigating the properties of high mass stars. The special distribution of open clusters yield a useful probe of the structure of the Galactic disk: the youngest systems probe the spiral structure of the Galaxy, while the older systems trace the kinematics of the outer Galaxy. Since it is believed that many stars in the disk of Milky Way originated in open clusters, the properties of these systems must dictate many of the properties of the stellar disk population as a whole (Binney and Merrifield, 1998).

4.1 Proper Motion and Membership Discussion of the Clusters

In this study, we used the data from the UCAC4 catalogue of individual stars detected in the field of view (FOV) of the clusters. The fourth United States Naval Observatory (USNO) CCD Astrograph catalogue, UCAC4, ware introduced by Zacharias et al. (2013). The catalogue presents data of more than one thousand million objects covering the entire sky. The magnitude limit of the objects is up to 16 mag in filter *R*. The reference star positions in UCAC4 are accurate to about 0.02 for brighter stars (10-14 mag), and an accuracy better than 0.1 is expected at the limiting magnitude of 16 mag. The systematic errors in the proper motions are estimated to be the order of 1 to 4 mas/yr. Dias et al. (2014) reported about the proper motions of the open clusters based on the UCAC4 catalogue. Accurate coordinates (RA, Dec), magnitudes in B, V, J, K and proper motions for the stars in the FOV were extracted from the UCAC4 catalogue. The VizieR tool is used in the catalogue. The apparent diameter and central coordinates of the cluster were taken from the DAML02 catalogue. However, some observed stars were not found in this catalogue. A programme to perform the astrometric calibration of the various CCD fields was used (courtesy of Dr T. Pauwels, ROB). The proper motions of the stars in FOV are considered for a discussion about their cluster membership probability.

4.1.1 Proper Motion of NGC 2126

We used the data from the UCAC4 catalogue of 442 individual stars detected in the FOV of NGC 2126. Figure 4.1 presents the proper motion vector-point diagram of all stars in the FOV in units of mas/yr. In order to minimize the effect of the high proper-motion field stars, we restricted the analysis to the range $|\mu| < 30$ mas/yr following Wu et al. (2002). Figure 4.2 presents the proper motion vector-point diagram of the stars with $|\mu| < 30$ mas/yr. The distributions of proper motion in RA and Dec are fitted with Gaussian function to measure the average value of the cluster as shown in Figure 4.3 and Figure 4.4, respectively. As a result, the average proper motion of NGC 2126: $\mu_\alpha \cos\delta$ = 0.36±0.20 mas/yr and μ_δ = -2.21±0.23 mas/yr. The average values are close to zero, therefore the cluster members are not easily distinguishable in proper motion from the background stars.

4.1.2 A High Proper Motion Star in NGC 2126

LHS 1809 ($RA_{2000} = 06^h02^m29^s$, $Dec_{2000} = +49^{\circ}52'56''$) is a high proper motion star from a catalogue of northern stars with annual proper motions larger than 0.15″ (LSPM-NORTH Catalogue) (Lépine and Shara, 2005) with spectral type M5V (Wenger et al., 2000). The position of LHS 1809 is located at the right part of CMD in the group of M dwarf stars. From the results of our astrometric analysis, the proper motion of the LHS 1809 is $\mu_\alpha \cos\delta = 115.7$ mas/yr and $\mu_\delta = -823.7$ mas/yr. Due to the high value of proper motion, it is a foreground object located between the cluster and the Sun/Earth.

4.1.3 Proper Motion of NGC 1528

We used the data from the UCAC4 catalogue of 270 stars detected in the FOV of NGC 1528. Figure 4.5 presents the proper motion vector-point diagram of all stars in the FOV in units of mas/yr. In order to minimize the effect of the high proper-motion field stars, we restricted the analysis to the range $|\mu| < 30$ mas/yr following Wu et al. (2002). Figure 4.6 presents the proper motion vector-point diagram of the stars with $|\mu| <$ 30 mas/yr. The distributions of proper motion in RA and Dec are fitted with Gaussian function to measure the average value of the cluster as shown in Figure 4.7 and Figure 4.8, respectively. As a result, the average proper motion of NGC 1528: $\mu_\alpha \cos\delta$ = 1.40±0.20 mas/yr and μ_δ = -1.75±0.20 mas/yr. The average values are close to zero, therefore the cluster members are not easily distinguishable in proper motion from the background stars.

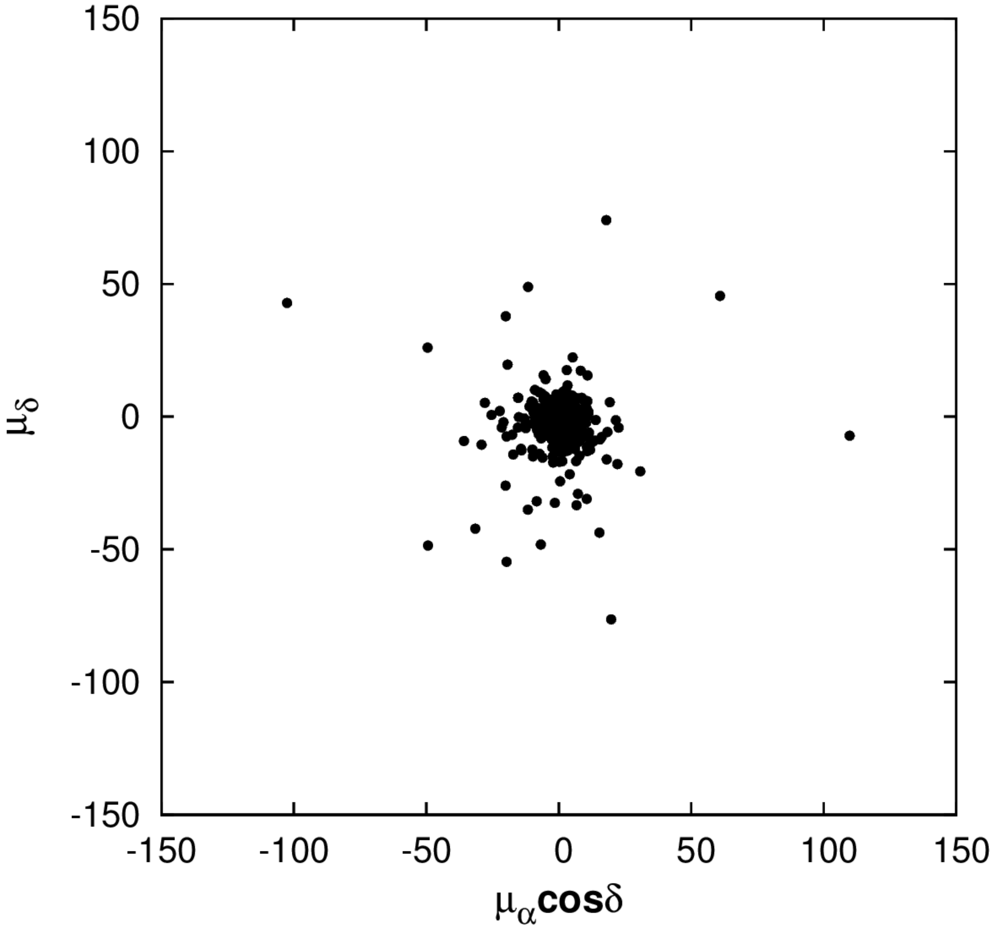

Figure 4.1: The proper motion vector-point diagram of all stars in the FOV of NGC 2126 (units are mas/yr).

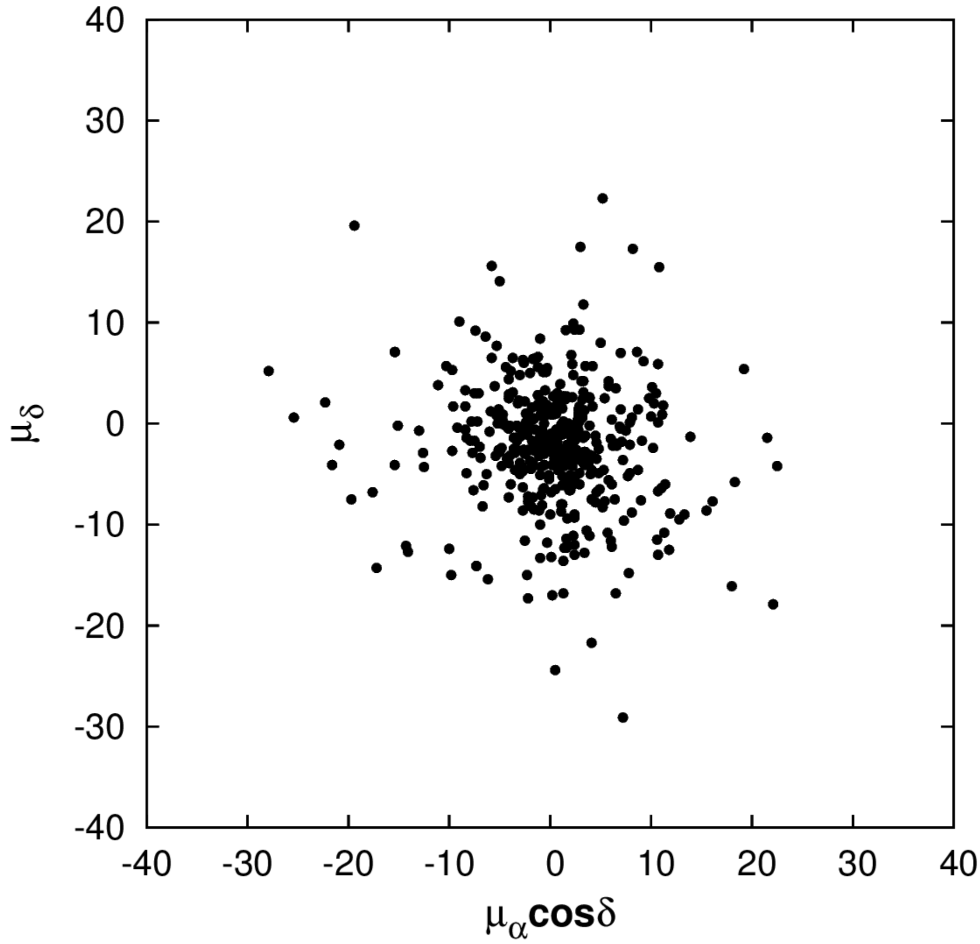

Figure 4.2: The proper motion vector-point diagram of the stars in NGC 2126 and field stars (units are mas/yr). Only the stars with $|\ \mu\ | < 30$ mas/yr were plotted.

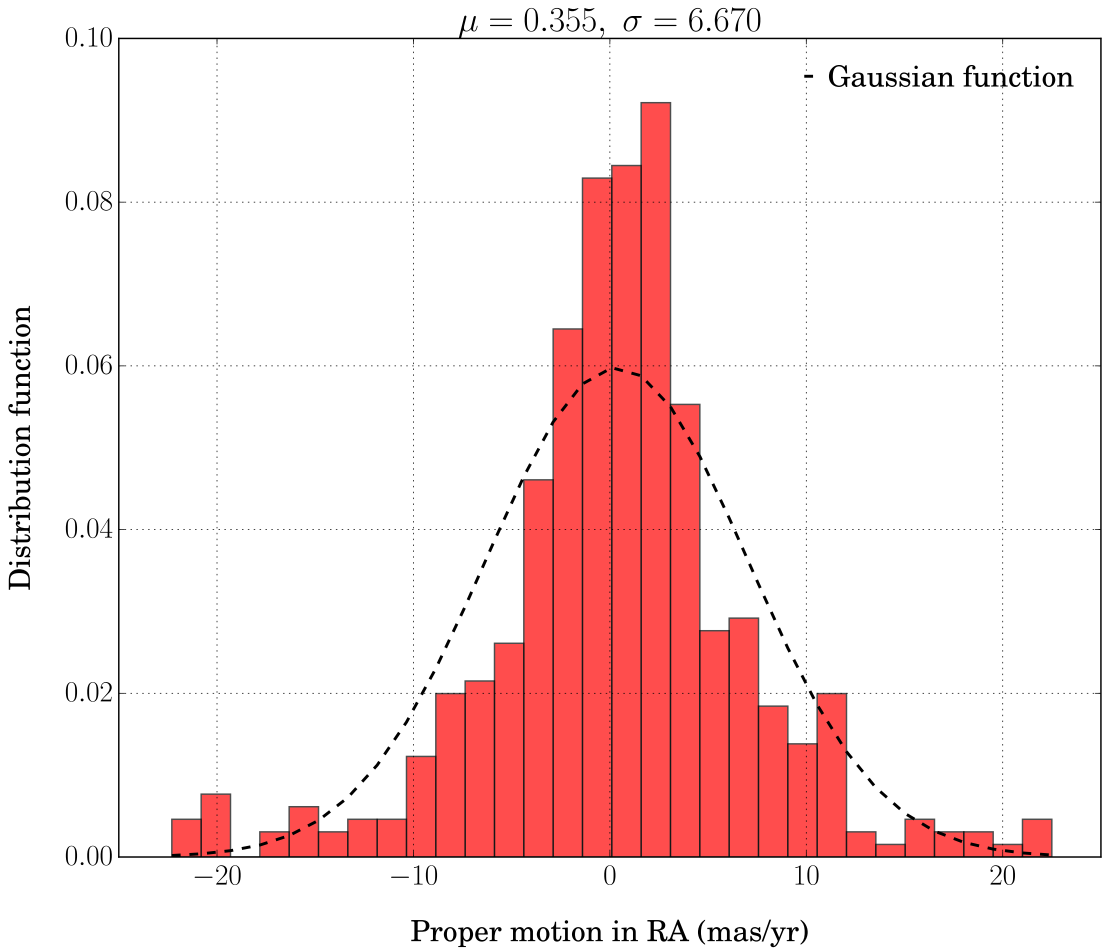

Figure 4.3: Distribution of proper motion in RA (mas/yr) of NGC 2126 fitted with Gaussian function.

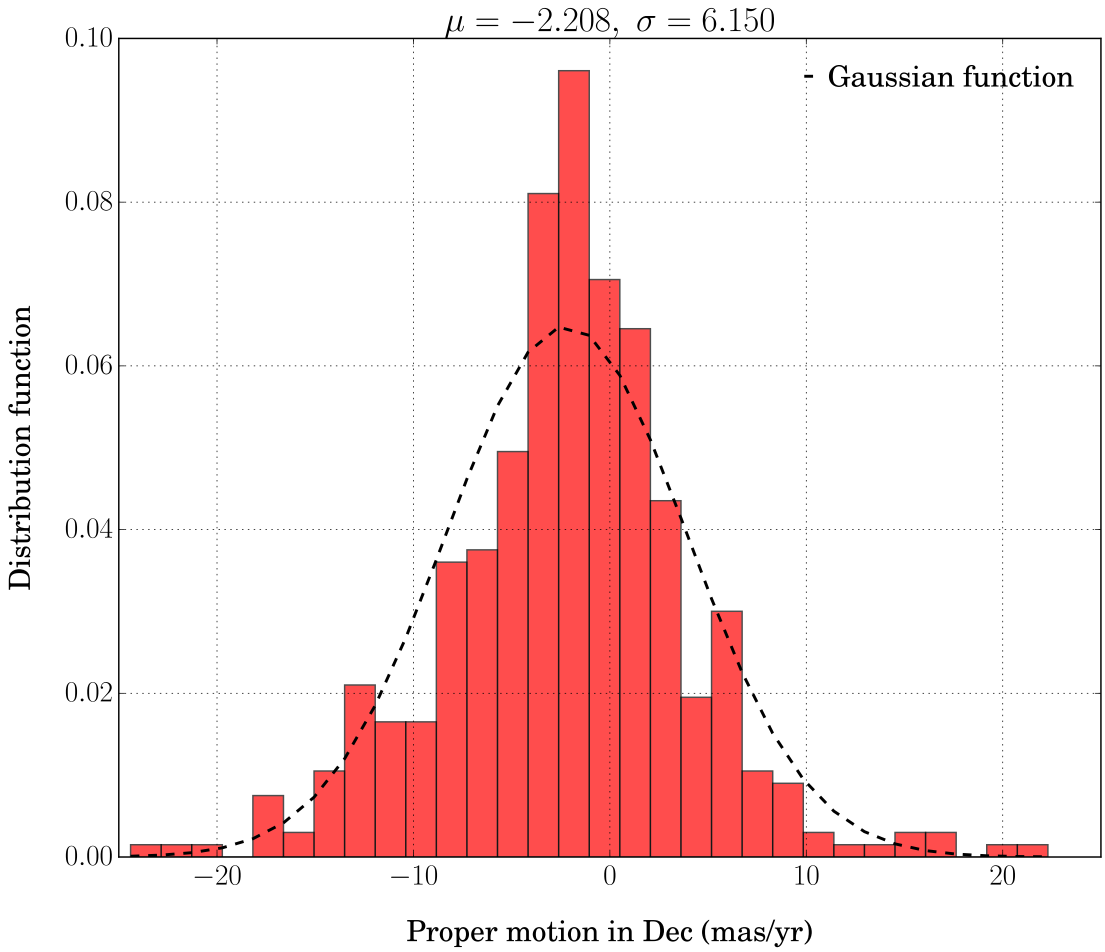

Figure 4.4: Distribution of proper motion in Dec (mas/yr) of NGC 2126 fitted with Gaussian function.

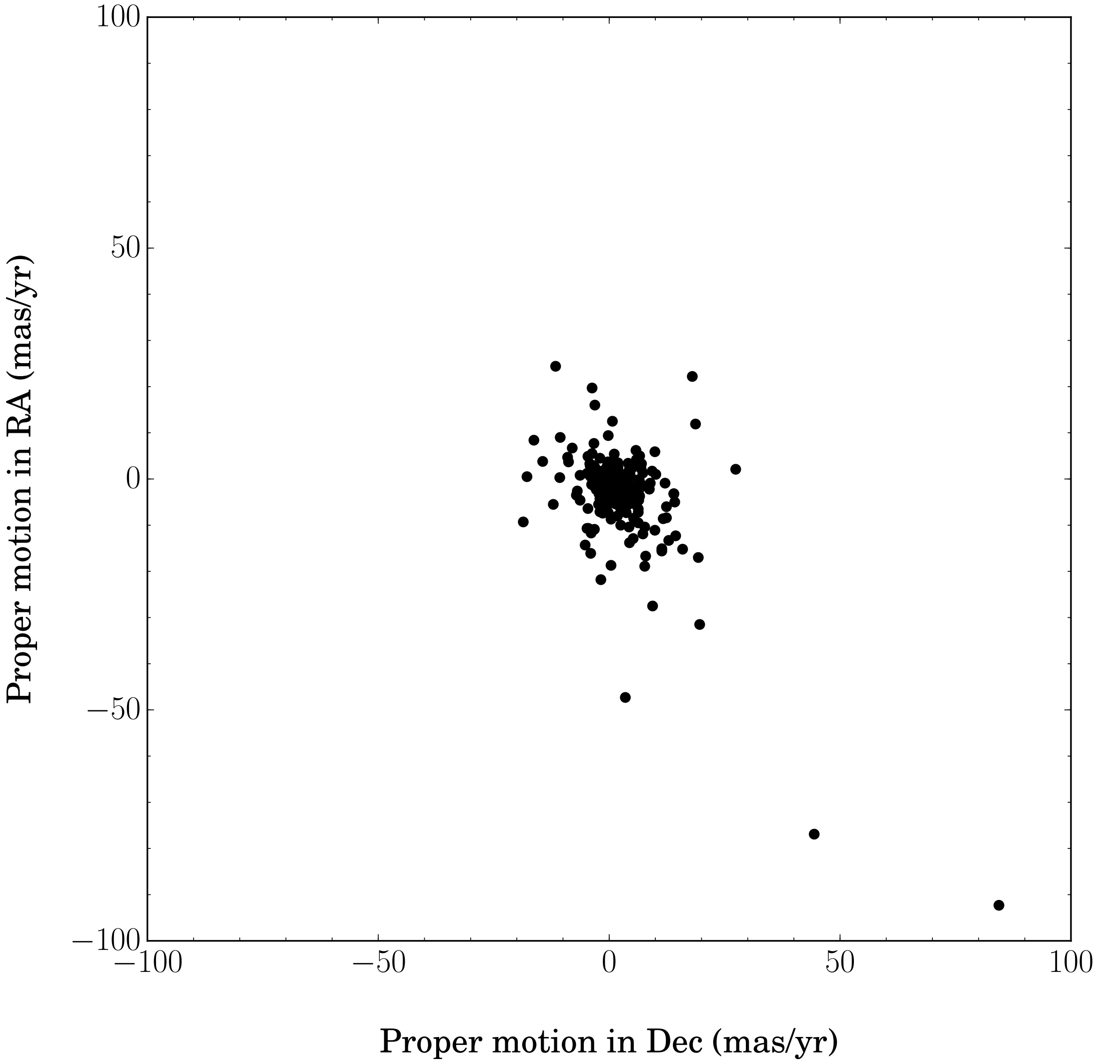

Figure 4.5: The proper motion vector-point diagram of all stars in the FOV of NGC 1528 (Units are mas/yr).

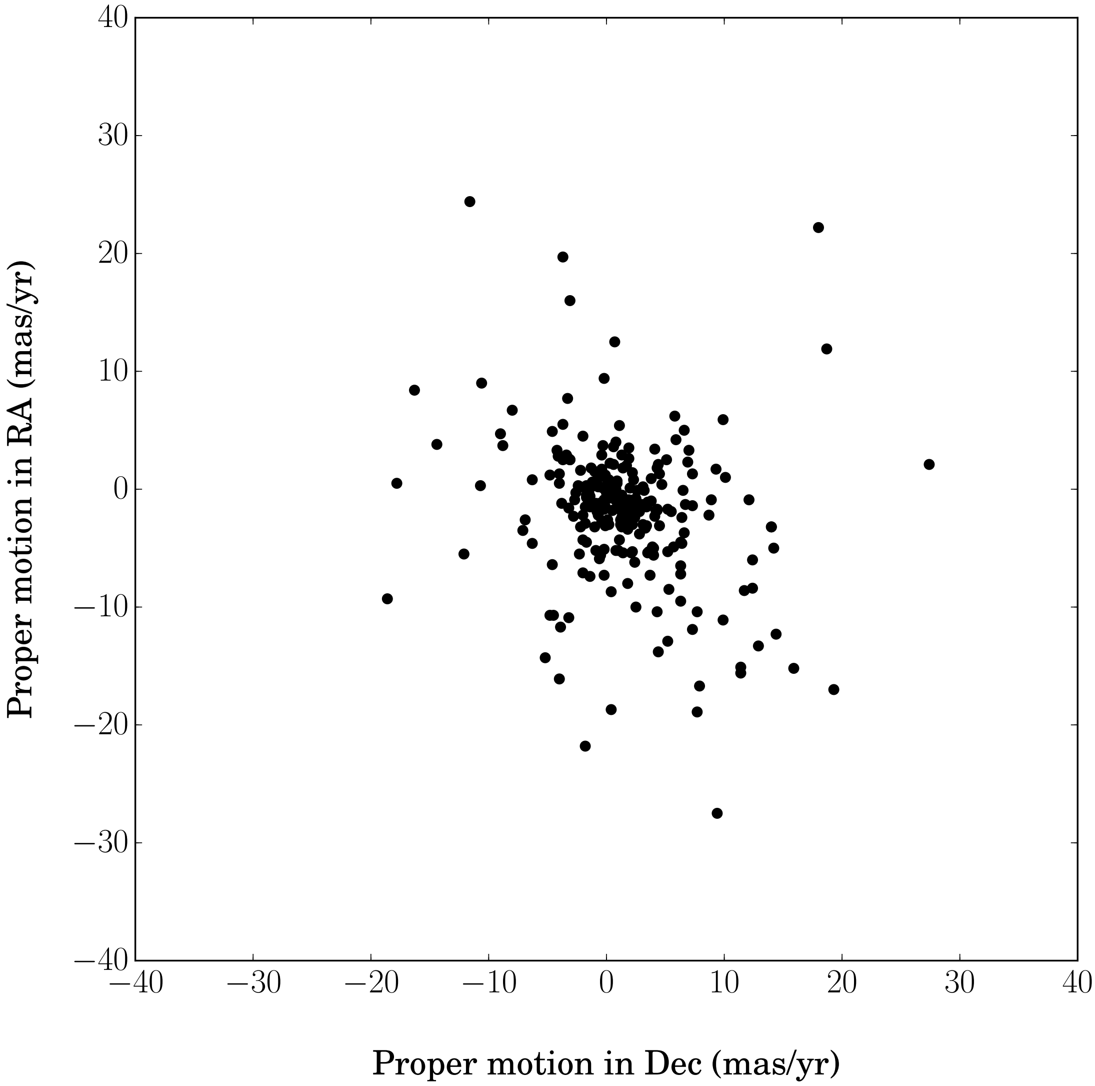

Figure 4.6: The proper motion vector-point diagram of the stars in NGC 1528 and field stars (Units are mas/yr). Only the stars with $\mid \mu \mid < 30$ mas/yr were plotted.

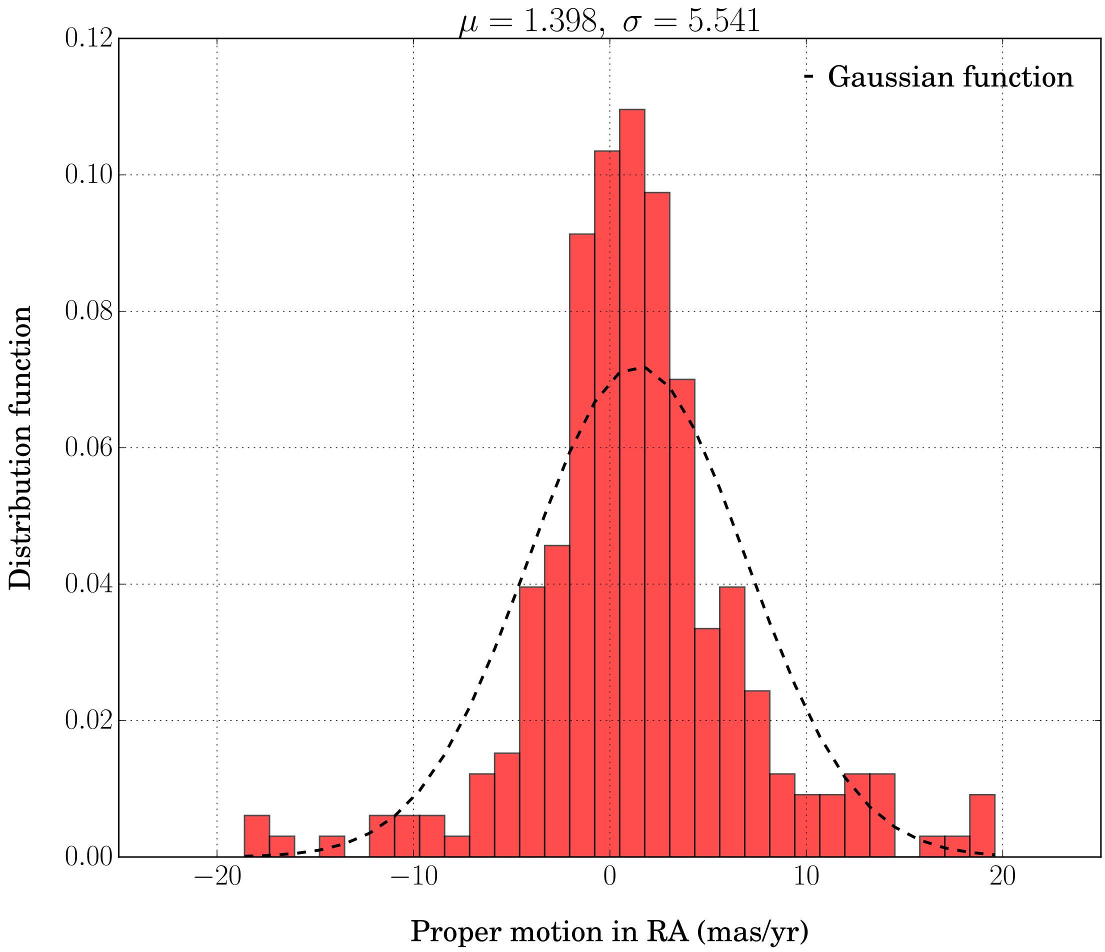

Figure 4.7: Distribution of proper motion in RA (mas/yr) of NGC 1528 fitted with Gaussian function.

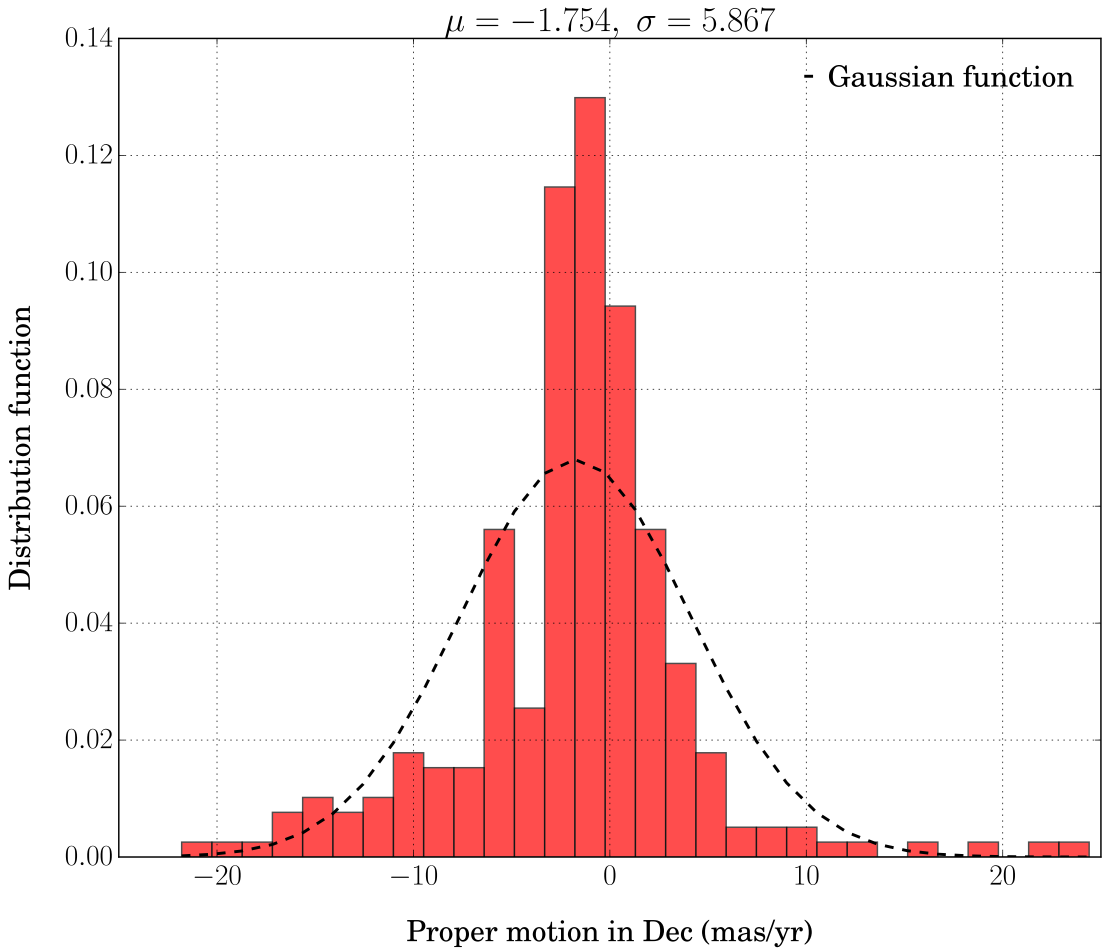

Figure 4.8: Distribution of proper motion in Dec (mas/yr) of NGC 1528 fitted with Gaussian function.

4.2 Colour Magnitude Diagram (CMD) and Parameters of the Clusters

4.2.1 CMD and Parameters of NGC 2126

We measured the instrumental magnitudes of various stars in M67 (RA = $08^{h}51^{m}18^{s}$, Dec. = $+11°48'$). This reference cluster was observed on 8th February 2013 and computed the transformation coefficients from the standard stars. The instrumental and standard magnitudes in B and V bands of stars in M67 are presented in Table 4.1. The transformation equations are

$$B - V = 0.977(b - v) - 0.418. \tag{4.1}$$

$$V - v = -0.012(b - v) - 0.692. \tag{4.2}$$

The CMD of the cluster (see Figure 4.9) presents a scattered look which makes it difficult to identify the stars on the ZAMS. The cluster appears to be rather young and no giant stars seem to be present in our sample. We computed the theoretical isochrones with the PAdova and tRieste Stellar Evolution Code from the PARSEC database (Bressan et al., 2012). To allow for the comparison between observations and theoretical isochrones, we fixed the distance modulus to $(m - M)$ = 11.25 mag. Figure 4.9 represents the best fit isochrone of the cluster. We found that the shape of the CMD at the turn-off point is well reproduced with an isochrone of log(t) of 9.1$\pm$0.1 yr and a metallicity of 0.019. $E(B-V)$ = 0.27$\pm$0.01 mag and $(m-M)_0$ = 10.80$\pm$0.05 mag. The fundamental properties for NGC 2126 determined in this study are summarized in Table 4.2. We also compared our result with those reported by Gáspár et al. (2003), Liu et al. (2009), Zhang et al. (2012). In general, our values are in good agreement with those from Gáspár et al. (2003). However, we observe significant differences with the results from Liu et al. (2009) and Zhang et al. (2012).

Table 4.1: Instrumental and standard magnitudes of stars in the reference cluster M67

No.	RA(2000)	Dec(2000)	b	v	b-v	B	V	B-V
1	08:51:16.8	11:48:00	12.733	11.002	1.731	11.555	10.289	1.266
2	08:51:24.0	11:48:00	12.739	11.172	1.567	11.562	10.453	1.109
3	08:51:26.4	11:48:36	12.219	11.198	1.021	11.065	10.489	1.109
4	08:51:21.6	11:46:12	13.657	12.132	1.525	12.501	11.427	1.074
5	08:51:24.0	11:49:48	13.543	12.206	1.337	12.370	11.485	0.885
6	08:51:19.2	11:46:48	13.735	12.838	0.897	12.573	12.116	0.457
7	08:51:21.6	11:45:36	13.965	12.948	1.017	12.824	12.253	0.571
8	08:51:16.8	11:45:36	14.275	13.086	1.189	13.136	12.391	0.745
9	08.51:19.2	11:49:48	14.269	13.241	1.028	13.125	12.528	0.587
10	08:51:26.4	11:47:24	14.275	13.243	1.032	13.130	12.540	0.590
11	08:51:19.2	11:46:48	14.510	13.279	1.231	13.361	12.580	0.781
12	08:51:19.2	11:49:12	14.399	13.348	1.051	13.246	12.640	0.606
13	08:51:14.4	11:47:24	14.316	13.369	0.947	13.167	12.665	0.502
14	08:51:24.0	11:48:36	14.400	13.396	1.004	13.249	12.691	0.558
15	08:51:19.2	11:46:12	14.422	13.418	1.004	13.284	12.724	0.560
16	08:51:19.2	11:46:48	14.462	13.467	0.995	13.315	12.761	0.554
17	08:51:14.4	11:50:24	14.480	13.485	0.995	13.350	12.790	0.560
18	08:51:28.8	11:49:12	14.464	13.570	0.894	13.257	12.796	0.461
19	08:51:24.0	11:48:36	14.547	13.530	1.017	13.387	12.815	0.572
20	08:51:14.4	11:47:24	14.527	13.522	1.005	13.379	12.821	0.558
21	08:51:21.6	11:46:12	14.482	13.593	0.889	13.343	12.891	0.452
22	08:51:28.8	11:45:36	14.914	13.558	1.356	13.832	12.906	0.926

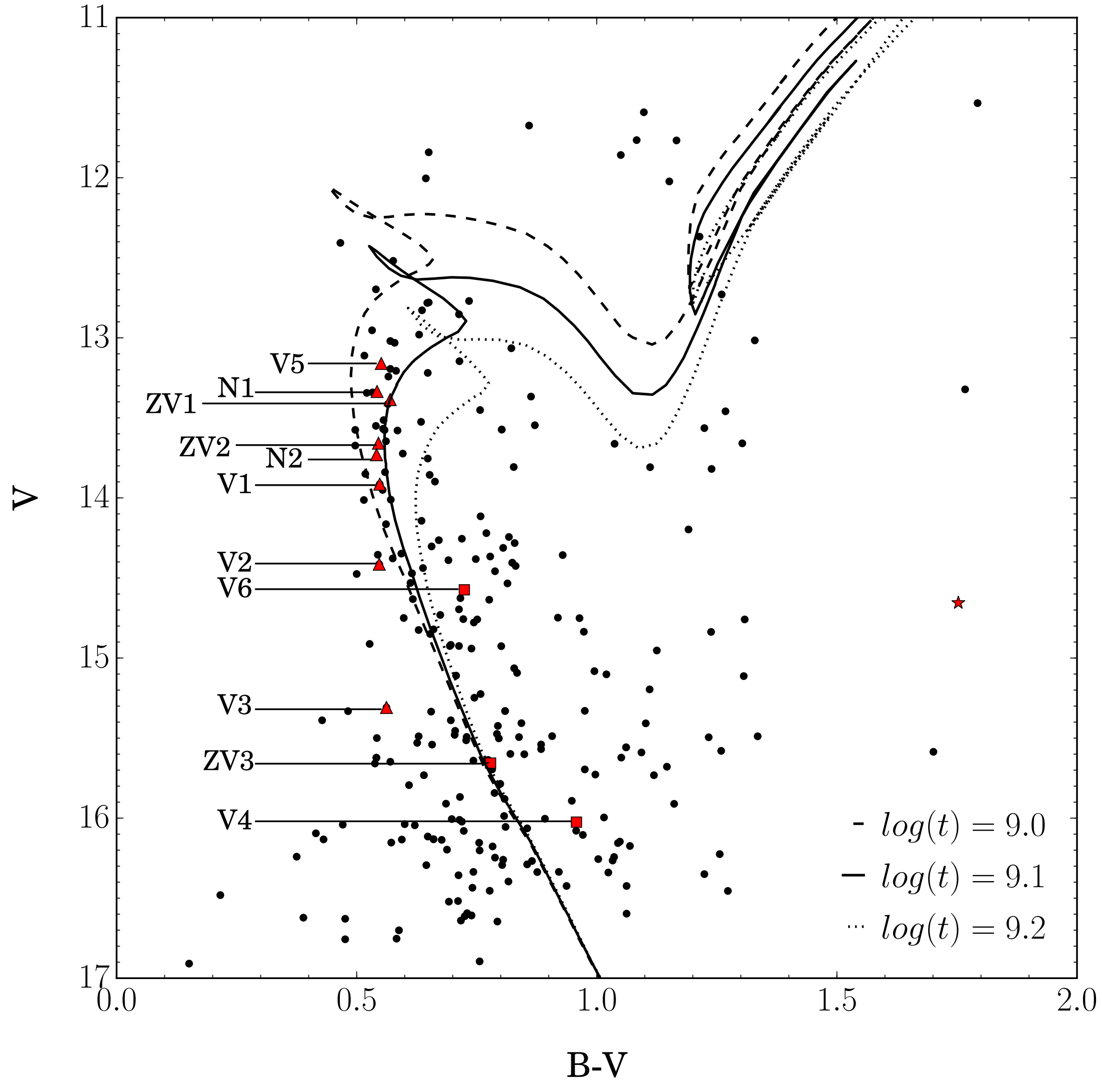

Figure 4.9: Colour-magnitude diagram for the stars in NGC 2126. Red filled triangles represent the pulsating stars, red filled squares represent eclipsing binary systems and red star represents the high proper motion star in the cluster. Isochrones from Bressan et al. (2012) are plotted with dashed line, full line and dot-dashed line for log(age) = 9.0, 9.1 and 9.2 yrs, respectively.

Table 4.2: Physical parameters of the open cluster NGC 2126

Reference	$E(B-V)$ (mag)	$(m-M)_v$ (mag)	log (t) (yrs)	[Fe/H]	$(m-M)_0$ (mag)	d (kpc)
Gáspár et al. (2003)	0.2±0.15	-	9.10	0.019	11± 0.6	1.3
Liu et al. (2009)	0.55	-	8.95	0.008	10.34	-
Zhang et al. (2012)	0.38±0.02	11.25 ± 0.05	9.10	0.008	10.01±0.05	1
This study	0.27±0.01		9.1	0.019	10.80±0.05	1.4

4.2.2 CMD and Parameters of NGC 1528

For the open cluster NGC 1528, accurate coordinates (RA, Dec), magnitudes in B and V of the stars in the FOV were extracted from the UCAC4 catalogue. We computed the theoretical isochrones with the PAdova and tRieste Stellar Evolution Code from the PARSEC database (Bressan et al., 2012). Figure 4.10 represents the best fit isochrone of the cluster. We found that the shape of the CMD at the turn-off point is well reproduced with an isochrone of log(t) of 8.50±0.05 yr and a metallicity of 0.019. $E(B-V)$ = 0.25±0.01 mag and $(m-M)_0$ = 9.85±0.05 mag.

Table 4.3: Coordinates in RA and Dec, UCAC4 catalogue names and magnitudes of the stars in NGC 1528

WEBDA ID	RA(2000)	Dec(2000)	UCAC4 name	B	V	B-V
1	4:14:57.156	+51:13:56.36	707-030040	9.203	8.991	0.212
2	4:15:09.755	+51:14:49.08	707-030100	9.901	9.660	0.241
3	4:15:22.357	+51:11:26.30	706-029706	10.219	9.962	0.257
4	4:15:10.152	+51:11:40.51	706-029667	10.937	10.026	0.911
5	4:15:19.710	+51:14:23.38	707-030144	11.250	10.098	1.152
6	4:14:46.183	+51:12:52.75	707-030003	10.734	10.105	0.629
7	4:14:46.732	+51:08:04.83	706-029606	10.484	10.129	0.355
8	4:15:40.616	+51:20:32.53	707-030239	10.718	10.423	0.295
9	4:14:54.779	+51:09:44.22	706-029627	10.802	10.415	0.387
10	4:15:46.003	+51:10:00.42	706-029796	11.071	10.817	0.254
11	4:15:46.691	+51:10:54.74	706-029798	11.473	11.217	0.256
12	4:15:17.338	+51:09:59.76	706-029688	11.589	11.307	0.282
13	4:15:56.543	+51:12:09.28	707-030310	11.644	11.339	0.305
14	4:15:43.633	+51:14:46.79	707-030247	12.355	11.982	0.373
15	4:15:32.543	+51:11:07.09	706-029742	12.951	12.497	0.454
16	4:15:42.211	+51:10:55.08	706-029776	12.937	12.555	0.382
17	4:15:37.112	+51:12:45.76	707-030221	13.069	12.608	0.461
18	4:15:52.326	+51:11:28.75	706-029824	13.088	12.72	0.368
19	4:15:20.719	+51:13:34.55	707-030148	13.632	13.044	0.588
20	4:15:28.205	+51:13:45.69	707-030183	13.773	13.291	0.482
21	4:14:42.183	+51:10:51.48	706-029591	14.096	13.364	0.732
22	4:14:46.499	+51:12:03.55	707-030005	14.277	13.528	0.749
23	4:15:07.338	+51:11:54.05	706-029657	14.170	13.604	0.566
24	4:15:37.703	+51:07:46.12	706-029754	14.997	14.039	0.958
25	4:15:40.217	+51:09:24.97	706-029769	15.032	14.335	0.697
26	4:15:11.022	+51:12:38.83	707-030108	15.222	14.341	0.881
27	4:15:34.401	+51:08:16.33	706-029746	15.139	14.406	0.733
28	4:14:42.114	+51:11:57.69	706-029590	15.566	14.823	0.743
29	4:15:53.889	+51:13:41.84	707-030305	15.769	14.925	0.844
30	4:15:14.392	+51:12:18.97	707-030124	16.292	15.455	0.837
31	4:15:51.355	+51:06:55.98	706-029819	9.939	9.480	0.459
32	4:14:55.224	+51:10:42.45	706-029630	11.535	10.072	1.463
33	4:15:51.376	+51:16:29.38	707-030284	10.554	10.226	0.328
34	4:15:21.936	+51:12:48.11	707-030153	10.798	10.497	0.301
35	4:15:44.005	+51:07:15.78	706-029786	11.122	10.495	0.627
36	4:16:04.662	+51:12:10.70	707-030341	10.996	10.775	0.221
37	4:15:25.590	+51:12:11.80	707-030172	11.218	10.976	0.242
38	4:15:50.052	+51:09:30.76	706-029811	11.366	11.103	0.263
39	4:15:16.155	+51:09:21.74	706-029686	11.344	11.047	0.297
40	4:15:39.880	+51:19:05.46	707-030238	11.491	11.207	0.284

Table 4.4: Coordinates in RA and Dec, UCAC4 catalogue names and magnitudes of the stars in NGC 1528 (continued)

WEBDA ID	RA(2000)	Dec(2000)	UCAC4 name	B	V	B-V
41	4:15:33.812	+51:11:31.04	706-029745	11.579	11.278	0.301
42	4:15:25.245	+51:16:28.95	707-030169	11.760	11.348	0.412
43	4:15:12.202	+51:17:35.36	707-030112	11.635	11.387	0.248
44	4:16:19.445	+51:07:59.57	706-029934	11.502	11.290	0.212
45	4:15:51.288	+51:08:46.66	706-029818	11.828	11.443	0.385
46	4:15:20.748	+51:09:06.67	706-029698	11.713	11.373	0.340
47	4:15:52.085	+51:17:06.85	707-030287	11.817	11.515	0.302
48	4:15:21.011	+51:11:47.65	706-029700	11.874	11.594	0.280
49	4:15:30.278	+51:13:05.93	707-030191	11.984	11.760	0.224
50	4:16:14.348	+51:09:11.53	706-029916	12.421	11.912	0.509
51	4:15:41.607	+51:18:37.24	707-030241	12.271	11.984	0.287
52	4:15:31.947	+51:14:56.67	707-030204	12.723	12.040	0.683
53	4:15:42.079	+51:17:37.73	707-030242	12.599	12.280	0.319
54	4:14:44.506	+51:13:41.83	707-029997	12.738	12.347	0.391
55	4:15:54.826	+51:09:58.72	706-029835	12.949	12.374	0.575
56	4:15:47.841	+51:14:05.01	707-030266	13.920	12.583	1.337
57	4:15:35.635	+51:15:30.42	707-030215	12.785	12.422	0.363
58	4:14:52.601	+51:10:56.54	706-029619	12.781	12.366	0.415
59	4:16:12.898	+51:08:04.49	706-029911	12.950	12.608	0.342
60	4:16:05.538	+51:14:51.15	707-030344	13.236	12.599	0.637
61	4:15:53.356	+51:12:28.46	707-030302	13.187	12.645	0.542
62	4:15:58.074	+51:12:44.03	707-030318	13.908	12.759	1.149
63	4:15:27.385	+51:11:38.50	706-029728	13.126	12.700	0.426
64	4:15:2.598	+51:16:22.11	707-030068	13.452	12.732	0.720
65	4:15:38.360	+51:18:16.29	707-030229	13.054	12.69	0.364
66	4:14:53.428	+51:14:36.33	707-030025	13.110	12.751	0.359
67	4:16:16.282	+51:07:29.85	706-029921	13.002	12.654	0.348
68	4:16:01.079	+51:09:30.56	706-029859	13.145	12.703	0.442
69	4:15:41.807	+51:07:30.56	706-029774	13.253	12.75	0.503
70	4:15:03.162	+51:17:45.56	707-030072	13.237	12.809	0.428
:	:	:	:	:	:	:
:	:	:	:	:	:	:
:	:	:	:	:	:	:
1508	4:16:42.424	+51:15:07.47	707-030481	13.116	12.552	0.564
1510	4:16:43.621	+51:10:40.57	706-030008	14.110	13.552	0.558
1511	4:16:43.360	+51:14:36.61	707-030485	15.912	14.986	0.926
1513	4:16:43.461	+51:16:35.95	707-030487	13.571	12.953	0.618
1516	4:16:45.424	+51:07:34.71	706-030016	14.374	13.695	0.679

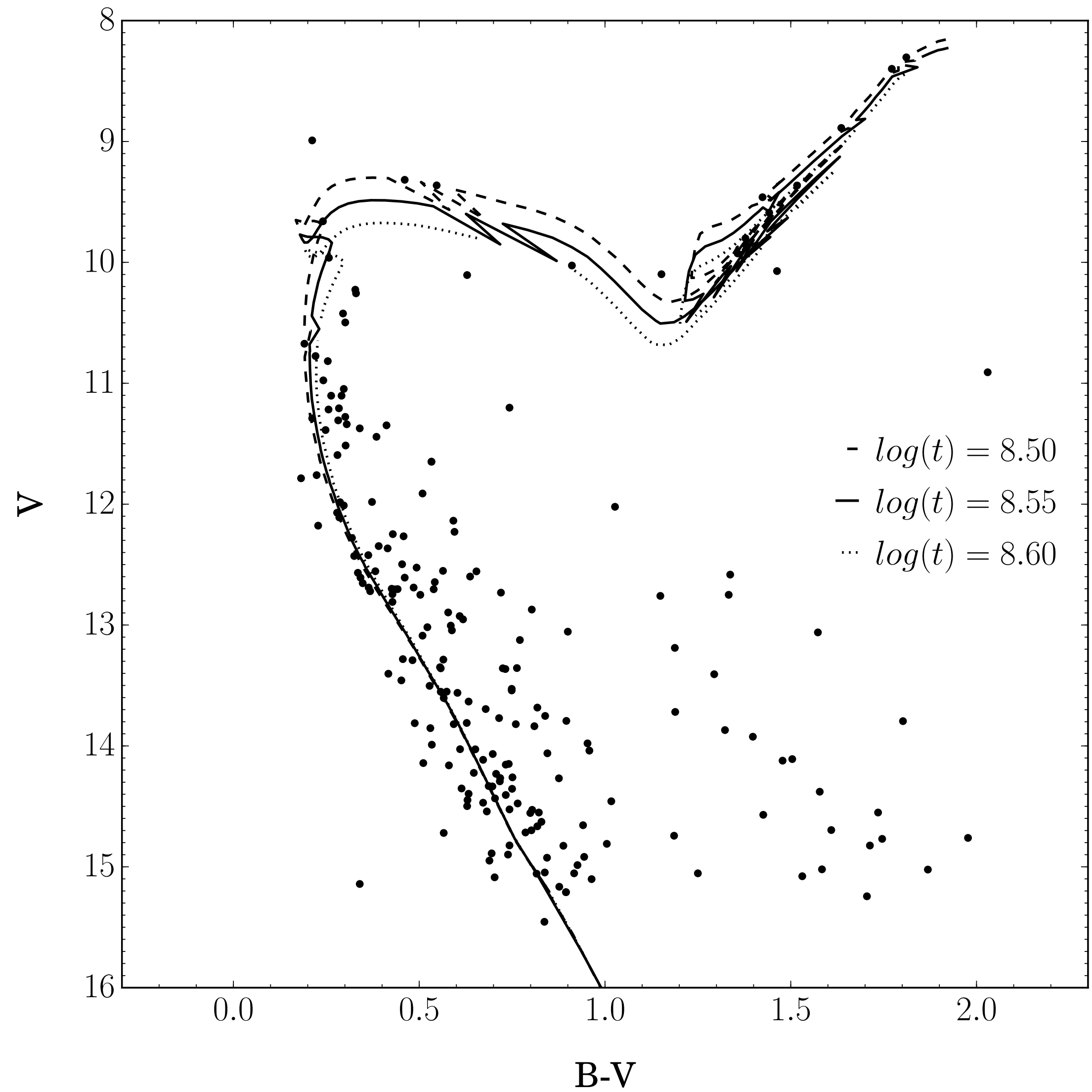

Figure 4.10: Colour-magnitude diagram for the stars in NGC 1528. Isochrones from Bressan et al. (2012) are plotted with dashed line, full line and dot-dashed line for log(age) = 8.50, 8.55 and 8.60 yrs, respectively.